Signaling Mechanisms of HAMP Domains in Chemoreceptors and Sensor Kinases

John S. Parkinson

Biology Department, University of Utah, Salt Lake City, Utah 84112;
email: parkinson@biology.utah.edu

Annu. Rev. Microbiol. 2010. 64:101–22

First published online as a Review in Advance on May 12, 2010

The *Annual Review of Microbiology* is online at micro.annualreviews.org

This article's doi:
10.1146/annurev.micro.112408.134215

0066-4227/10/1013-0101$20.00

Key Words

transmembrane signaling, conformational coupling, phase clash, dynamic bundle, piston model

Abstract

HAMP domains mediate input-output signaling in histidine kinases, adenylyl cyclases, methyl-accepting chemotaxis proteins, and some phosphatases. HAMP subunits have two 16-residue amphiphilic helices (AS1, AS2) joined by a 14- to 15-residue connector segment. Two alternative HAMP structures in these homodimeric signaling proteins have been described: HAMP(A), a tightly packed, parallel, four-helix bundle; and HAMP(B), a more loosely packed bundle with an altered AS2/AS2′ packing arrangement. Stimulus-induced conformational changes probably modulate HAMP signaling by shifting the relative stabilities of these opposing structural states. Changes in AS2/AS2′ packing, in turn, modulate output signals by altering structural interactions between output helices through heptad repeat stutters that produce packing phase clashes. Output helices that are too tightly or too loosely packed most likely produce kinase-off output states, whereas kinase-on states require an intermediate range of HAMP stabilities and dynamic behaviors. A three-state, dynamic bundle signaling model best accounts for the signaling properties of chemoreceptor mutants and may apply to other transducers as well.

Contents

INTRODUCTION

Microbes lead rich sensory lives. Their physical and chemical environments can undergo rapid and unpredictable changes, presenting both new nutritional opportunities and life-threatening challenges. Accordingly, bacteria and archaea employ a variety of sensory systems to monitor their living conditions and to elicit adaptive responses to environmental changes. These sensory systems must handle signaling tasks common to most biological signal transduction pathways: detection of an external stimulus, transmission of stimulus information across the cytoplasmic membrane, and conversion of that information to a signal that triggers a change in behavior or gene expression.

Many bacterial signaling proteins contain HAMP domain signaling motifs, so-called because they are found in histidine kinases (HKs), adenylyl cyclases, methyl-accepting chemotaxis proteins (MCPs), and some phosphatases (6, 59). In membrane-associated proteins, HAMP domains usually lie near the cytoplasmic side of the membrane, where they convert transmembrane and intracellular sensory inputs to output response signals. This review focuses on studies of HAMP domain structure and function in a few well-studied representatives of chemoreceptors and histidine kinases (**Figure 1**). All these signaling proteins function as homodimers, and HAMP domain signaling mechanisms are probably intimately tied to this structural organization.

The goal of this review is to present testable mechanistic models of HAMP function in the chemoreceptors Tar and Tsr and in the histidine kinase NarX, for which the experimental pictures are most complete. I also discuss Aer, HtrII, and EnvZ to illustrate mechanistic variations on HAMP signaling themes.

Tar and Tsr

These members of the MCP superfamily (2) mediate attractant responses to the amino acids aspartate (Tar) and serine (Tsr) in

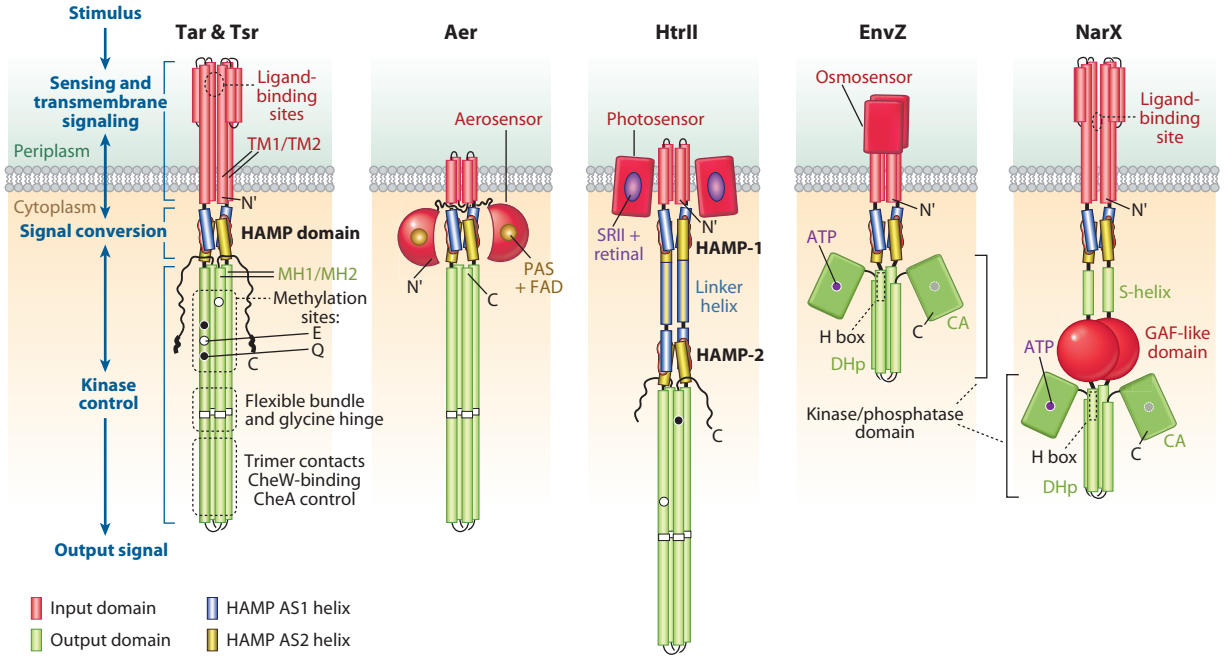

Figure 1

Chemoreceptors and sensor kinases discussed in this review. The cylindrical portions of the schematics, representing α-helical segments, are approximately to scale. The structural organization of domains and proteins that are not central to the review is not depicted. All these transducers function as homodimers. The C terminus of one subunit (C) and the N terminus of the other subunit (N′) are indicated. Black circles in the kinase control domains of Tar/Tsr and HtrII represent methylation sites synthesized as glutamines and subsequently deamidated to glutamates; white circles represent methylation sites synthesized as glutamates. Abbreviations: TM1, TM2, transmembrane segments 1, 2; MH1, MH2, methylation helices 1, 2; CA, catalytic and ATP-binding domain; DHp, dimerization and histidine-phosphotransfer domain; H box, segment containing the autophosphorylation site.

Escherichia coli (Ec) and in *Salmonella enterica* serovar Typhimurium (St) (reviewed in Reference 32). Chemoeffectors bind directly to the periplasmic sensing domains of these transducers, triggering conformational changes that are transmitted across the membrane through transmembrane helices (TM) joined to each HAMP subunit. The HAMP domain in turn connects to output methylation helices (MH1, MH1′) that comprise part of the receptor kinase control module. MH1 and MH1′ form an antiparallel four-helix bundle with their C-terminal counterparts (MH2, MH2′). The MH bundle contains sites of covalent modification for sensory adaptation (see below). Its membrane-distal tip promotes binding interactions with other receptors, with the histidine kinase CheA, and with CheW, which couples CheA activity to chemoreceptor control. Receptor signaling complexes are stable and regulate CheA autophosphorylation activity with high cooperativity. Phospho-CheA donates phosphoryl groups to two response regulators: CheY, for motor control, and CheB, for adaptation control. Phospho-CheY binds to the flagellar switch, enhancing the probability of clockwise (CW) rotation, which causes random changes in swimming direction. Counterclockwise (CCW) rotation, the default direction, produces forward-swimming episodes.

Tar and Tsr sense spatial chemical gradients temporally by comparing current ligand concentrations with those averaged over the past few seconds of the cell's travels. Ligand history is recorded in the form of methyl-group modifications at specific glutamyl residues in

HAMP: signaling motif found in histidine kinases, adenylyl cyclases, methyl-accepting chemotaxis proteins, and some phosphatases

MCP: methyl-accepting chemotaxis protein

TM: transmembrane helix

Four-helix bundle: a protein structure stabilized mainly through packing interactions between the hydrophobic faces of amphiphilic helices

PAS: a ubiquitous sensory input domain, often associated with a noncovalently bound cofactor; named for Per, ARNT, and SIM proteins of eukaryotes

Flavin adenine dinucleotide (FAD): a redox-sensing cofactor of the PAS domain in Aer

the MH bundle. When current and past conditions do not match, the receptor triggers a change in CheA activity to elicit an appropriate motor response. The stimulus also initiates a feedback loop that updates the receptor's methylation record to reflect current conditions so that the cell is poised to respond to any further chemical changes. Two competing enzymes control receptor methylation status: CheR, a methyltransferase, and CheB, a methylesterase/deamidase. CheR operates at fixed velocity, whereas CheB activity is greatly enhanced by phosphorylation. In addition, the signaling states of receptor molecules influence their substrate properties for the methylation and demethylation enzymes.

It is convenient to consider two receptor signaling states, a kinase-activating (ON or CW) state and a kinase-deactivating (OFF or CCW) state. Changes in ligand occupancy drive receptors toward one output state or the other to initiate behavioral responses, and subsequent changes in methylation state restore the prestimulus balance of the two states to achieve sensory adaptation.

Aer and HtrII

Aer is an MCP-like protein that mediates aerotactic behavior in *E. coli* and *S. enterica* (8, 42). The Aer molecule has a cytoplasmic MH bundle and protein interaction tip similar to those of Tar and Tsr, but it lacks methylation sites for sensory adaptation (9). Nevertheless, cells expressing Aer as their sole transducer do adapt to aerotactic stimuli; the underlying mechanism is unknown (52). Aer has no periplasmic sensing domain, but rather a cytoplasmic N-terminal PAS domain that binds flavin adenine dinucleotide (FAD) (7, 8, 43). The FAD cofactor functions as a redox sensor of electron transport activity (52). Changes in the level of oxygen or another electron acceptor shift the redox state of the PAS/FAD domain, which transmits that sensory information to the HAMP domain, which in turn modulates the kinase control output domain.

HtrII is an MCP-like phototransducer that has been extensively studied in *Halobacterium salinarum* (Hs) and, more recently, in *Natronomonas pharaonis* (Np) (45). The HtrII molecule has an MCP adaptation and kinase control domain preceded by two HAMP domains, connected through a linker helix, and four TM segments. HtrII(Np) has no appreciable periplasmic domain, whereas HtrII(Hs) has an extensive periplasmic domain that has been implicated in chemical sensing (33). The TM segments of HtrII form a stable membrane complex with sensory rhodopsin II (SRII), a photosensor. SRII detects light stimuli centered around a wavelength of 500 nM and triggers a repellent (photophobic) locomotor response through HtrII.

EnvZ and NarX

EnvZ and NarX employ two-component signaling pathways to regulate target gene expression. Both sensors control the phosphorylation state of their cognate response regulator (OmpR and NarL, respectively) through competing kinase and phosphatase activities. It is convenient to regard them as two-state signaling devices: One output state has high autokinase and phosphotransfer activity, and the other has high phosphatase activity. Through a poorly understood mechanism, EnvZ monitors the osmolarity of the medium and regulates the relative expression levels of outer membrane porins. NarX has a periplasmic domain that senses extracellular nitrate and nitrite levels. Under anaerobic conditions, NarX controls expression of gene products needed to use nitrate and nitrite compounds as terminal electron acceptors. The ligand-binding signals traverse the membrane to the HAMP domain, which communicates with an adjoining coiled-coil segment (S-helix) that in turn feeds information to a GAF-like domain, which probably modulates NarX output signals. S-helices are widespread signaling motifs (4) whose signaling interactions with HAMP domains have been intensively studied only in the NarX system (48).

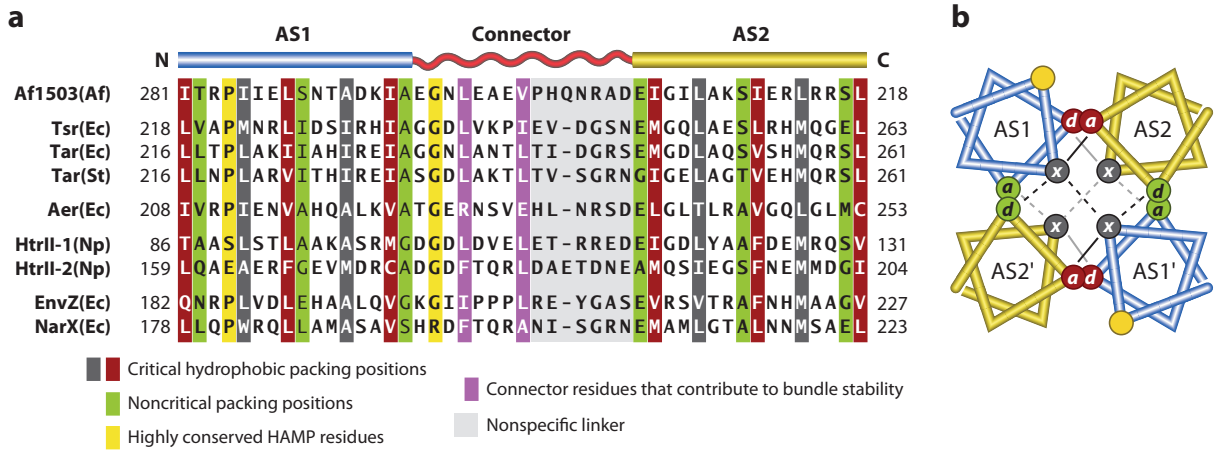

Figure 2

HAMP sequence features and bundle-packing arrangement. (*a*) Sequences of the HAMP domains discussed in this review. Af1503 is from *Archaeoglobus fulgidus* (Af); Tsr, Tar, Aer, EnvZ, and NarX are *Escherichia coli* (Ec) proteins; Tsr(St) is the Tar protein of *Salmonella enterica* serovar Typhimurium (St); HtrII-1 and HtrII-2 are two HAMP domains in HtrII from *Natronomonas pharaonis* (Np). Important residue positions are color-coded to the structure shown in panel *b*. The gray region of the connector functions as a nonspecific linker (3). (*b*) Helical wheels of the packing interactions promoted by the *x* and *a/d* residues positions in AS1 and AS2, viewed from the top (N termini) of the Af1503 four-helix bundle. Solid lines indicate intrasubunit interactions; dotted lines indicate intersubunit interactions. Two packing layers are shown: upper (*black*) and lower (*gray*).

HAMP STRUCTURES

HAMP motifs are defined by a few conserved residues, by characteristic hydrophobic heptad repeats, and by predicted helical and nonhelical secondary-structure elements (6, 15, 24, 59). HAMP subunits are ~50 residues long, with two predicted amphiphilic helices joined by a nonhelical connector (**Figure 2**). HAMP secondary-structure elements have been given diverse names, and their boundaries are also variously defined. The designations shown in **Figure 2** (AS1, AS2, CTR) correspond to those used for the serine receptor Tsr (3). The HAMP endpoints correspond to the first and last residues critical to HAMP function in Tsr (63).

HAMP(A): A Tight Four-Helix Bundle

Several years ago, Hulko et al. (34) reported a high-resolution NMR structure for a HAMP domain from a thermophile protein of unknown function (Af1503), an important breakthrough that has guided subsequent work on HAMP. The Af1503 HAMP structure revealed a parallel, four-helix bundle with each connector wrapped around the outside of the bundle in contact with the two helices from the same subunit (**Figure 3*a***). The AS1 and AS2 helices are offset by one helical turn in the bundle, with principal packing interactions between the characteristic heptad repeat hydrophobic residues (**Figure 2**). The defining residues in HAMP sequences occupy key positions in the Af1503 bundle structure (using Tsr numbering): P221 (AS1) and E248 (AS2) lie at the N terminus of the bundle, and A233 (AS1) lies at the C terminus of the bundle (**Figure 2*b*** and **Figure 3*a***). G235, a conserved residue at the start of the connector, makes a sharp turn in the structure (**Figure 3*a***); L237 and I241, although not strictly conserved connector residues, are typically hydrophobic amino acids whose side chains pack against the AS1 and AS2 helices to stabilize the bundle.

The Af1503 HAMP packing arrangement is unorthodox. A third position, usually occupied by a small, but not necessarily hydrophobic, residue (**Figure 2**) also contributes to bundle

Heptad repeats: repeating, seven-residue patterns of hydrophobic and nonhydrophobic residues in amphiphilic (or amphipathic) alpha-helices

AS1, AS2: amphiphilic helices (having a pronounced hydrophobic face) in HAMP subunits

CTR: a nonhelical connector segment in HAMP subunits

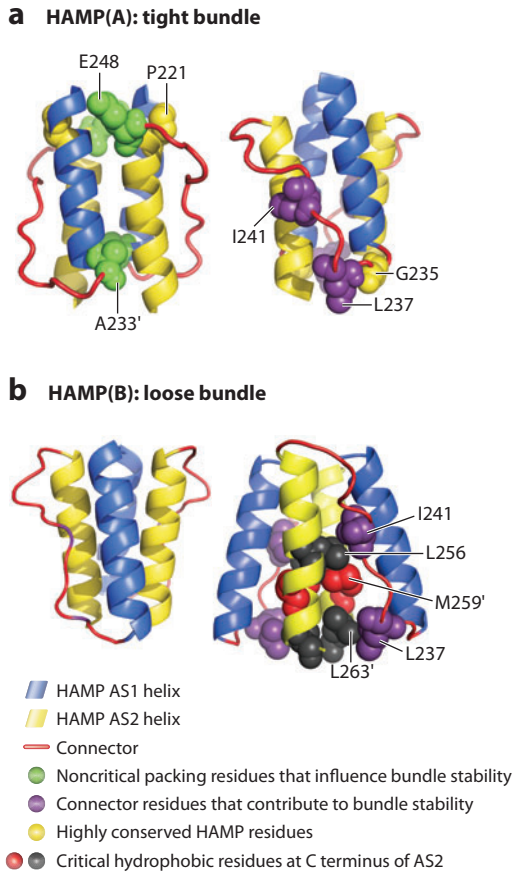

Figure 3

Two HAMP structures. The Tsr-HAMP sequence was threaded onto coordinates for Af1503 (34) and Aer2-HAMP2 (1); images were generated with PyMOL software. (*a*) Two side views of the Tsr-HAMP(A) bundle showing the register of AS1 and AS2 helices, key residues at the top and bottom of the bundle (*left*), and three key connector residues (*right*). Note that the connector lies in the groove between the AS1 and AS2 helices of the same subunit. (*b*) Two side views of the Tsr-HAMP(B) bundle showing the inward splay of AS2 helices and the outward splay of AS1 helices at the bottom of the bundle (*left*) and some key structural interactions at the C terminus of AS2 (*right*). Connector residue I241 interacts with L256 from the same subunit; connector residue L237 interacts with L263′ from the other subunit. The side chains of L256, L263, and M259 face toward the AS2/AS2′ interface.

packing. In this complementary *x-da*, or knobs-to-knobs, packing, the side chains of some hydrophobic residues project into the core of the bundle and make contact with their counterparts in the other subunit, whereas the side chains of the flanking hydrophobic residues interact with similar residues in the other helix of the same subunit (**Figure 2*b***). In contrast, the less hydrophobic packing positions (**Figure 2*b***) interact with similar residues in the other helix from the other subunit. This packing arrangement differs somewhat from the more commonly seen *a-d* or knobs-in-holes packing of coiled-coils, although a heptad repeat pattern of hydrophobic residues is common to both.

The Aer2 protein of *Pseudomonas aeruginosa* contains three sequential HAMP domains whose X-ray structures have recently been determined (1). Aer2-HAMP domains 1 and 3 have a bundle structure similar to that of Af1503-HAMP, but with further variations on the packing arrangements of the hydrophobic residues. These tight four-helix bundles, in which all AS1 and AS2 hydrophobic residues are intimately involved in bundle-stabilizing packing interactions, may represent a widely distributed HAMP structural state (1, 24), which I designate HAMP(A).

HAMP(B): A Loose Four-Helix Bundle

The HAMP-2 domain of Aer2 has a rather different structure that may represent a widespread alternative HAMP conformational state (1, 24). I denote this structure HAMP(B) and refer to it as a loose bundle. In the HAMP(B) structure the four helices have parallel orientations but are less tightly packed and splay apart from one another: AS1 and AS1′ are closest at the top of the bundle; AS2 and AS2′ are closest at the bottom of the bundle (**Figure 3*b***). Most importantly, the AS2/AS2′ helices pack against one another in a phase arrangement different from that in the HAMP(A) bundle, mainly through interactions between their three C-terminal hydrophobic residues (L256, M259, L263 in **Figure 3*b***). This alternative packing configuration is stabilized by the key hydrophobic connector residues: One (L237) packs against the last hydrophobic residue of AS2 from the other subunit (L263′); another (I241) packs against the first of the three C-terminal hydrophobic residues from the same subunit (L256).

HAMP STRUCTURES IN THE TRANSDUCERS

Tar and Tsr

Cysteine-scanning studies of the Tar(St) receptor in membrane preparations have provided the most direct information on HAMP structure in chemoreceptors, including the first evidence for amphiphilic helices in HAMP domains (15). A subsequent study, using predicted pairs of proximal and distal cysteine reporters, confirmed a four-helix bundle structure for Tar HAMP similar to that of Af1503 HAMP, but with somewhat different packing of the connector residues (49).

Mutational analyses of Tsr HAMP are also consistent with the HAMP(A) structure (3, 63). Tsr-HAMP residues critical for signaling function are the heptad repeat hydrophobic residues that promote AS1-AS2 packing interactions (63), the conserved proline near the start of AS1, the conserved alanine near the end of AS1, the conserved glutamate at the start of AS2 (63), the conserved glycine that forms the sharp turn at the beginning of the connector, and the two hydrophobic connector residues that pack against AS1 and AS2 side chains in the cleft between those helices (3) (see **Figure 2** and **Figure 3**). Many amino acid replacements at these critical HAMP positions impair or abolish Tsr signaling function, whereas all other HAMP positions tolerate a variety of amino acid replacements with no deleterious consequences. In addition, small, polar residues introduced at some of the critical hydrophobic packing positions in AS1 or AS2 are suppressible by residue changes in the same, or a contiguous, packing layer of the four-helix bundle (63). These suppression effects are allele specific, consistent with direct structural interactions between the deleterious and suppressor residues. Finally, dominance tests of HAMP lesions, particularly proline and arginine replacements at critical packing positions, distinguish most of the *x* residues from the critical *a/d* residues in the AS1 and AS2 helices, consistent with a bundle arrangement for Tsr HAMP in which the *x* and *a/d* residues play nonidentical packing roles (34, 63) (**Figure 2*b***).

Aer and HtrII

In vivo cysteine-directed cross-linking studies have shown that Aer HAMP contains two helical segments joined by a structured, but nonhelical, connector (56). In the native Aer dimer, the AS1 and AS2 helices form a four-helix bundle with principal packing interactions between hydrophobic residues at heptad repeat positions characteristic of the Af1503 bundle (56). However, the packing arrangement, inferred from disulfide-formation rates of predicted proximal and distal cysteine pairs, is not fully consistent with an *x-da* or *a-d* bundle (1; K. Watts, personal communication).

In vitro spectroscopy studies have provided some structural information for the first HtrII(Np) HAMP domain. There is no structural information for the second HtrII HAMP domain and there is little mutational information for this system. Spin-labeling distance measurements of an HtrII fragment containing HAMP-1 and the linker helix, reconstituted with SRII in membrane lipids, indicated that the HAMP-1 domain was in equilibrium between compact and dynamic conformations (21). The proportions of the two forms were influenced by ionic strength and temperature (11, 21), and the compact form was suggested to resemble the tight bundle of Af1503 HAMP (21). Trypsin cleaved a similar, solubilized HtrII fragment in the AS1 segment of HAMP-1, yielding a C-terminal fragment in which only the linker helix had a discernable NMR solution structure (31).

NarX and EnvZ

The sequence features (**Figure 2*a***) and mutant phenotypes of NarX HAMP are consistent with a four-helix bundle. Amino acid replacements in NarX have identified most of the same residues that play key structural roles in other HAMP bundles (5, 20). Although there has been no systematic mutational analysis of the EnvZ-HAMP domain, the available mutant evidence is at least consistent with a four-helix bundle structure. Mutations at several EnvZ residues that correspond to key positions in

Control cable: the segment that joins a transmembrane helix to the AS1 helix in each HAMP subunit; approximately 4–5 residues long; unknown secondary structure

the Af1503-HAMP bundle abrogate EnvZ signaling (36, 41, 65). Circular dichroism studies of EnvZ fragments containing the HAMP domain showed that those fragments were random or unstructured. Replacement with a more hydrophobic residue at one of the presumptive AS1 packing residues (A193L) conferred some secondary structure on the fragments, consistent with improved stability of a HAMP bundle (38).

HAMP SIGNALING MECHANISMS

Input Transmission via Control Cables

The most common route for sensory inputs to HAMP (used by Tar, Tsr, EnvZ, and NarX) involves transmission of stimulus-induced changes through helical TM segments. The key to understanding HAMP input control by this route appears to be the segment linking TM2 to AS1, which I call the control cable. The control cable corresponds to the section between the membrane-anchoring determinants of TM2 and the first critical residue of AS1. TM2 segments of transducers typically have one or more aromatic residues near their cytoplasmic end that partition at the lipid-water interface (22, 23). These are followed a few residues later by one or more basic residues that probably serve as stop-transfer signals during membrane insertion of the nascent receptor subunits. The side chains of those basic groups probably interact with negatively charged lipid head groups (40) but may not be embedded in the membrane (10). By these criteria, the control cables of Tar and Tsr are five residues in length; those of NarX and EnvZ appear to be one or two residues shorter.

Two plausible mechanisms of TM2-HAMP communication have been suggested: (*a*) a crankshaft and gearbox mechanism involving axial rotation of TM2 segments in the plane of the membrane (34), and (*b*) a piston mechanism involving displacements of TM2 segments perpendicular to the plane of the membrane (27, 28). The crankshaft and gearbox model arose from the suggestion that there should exist a more orthodox *a-d* packing alternative to the Af1503-HAMP *x-da* bundle, differing by an ~26° counterrotation of the four helices (34). If such a structure represented a different HAMP signaling state, then axial rotation of the connecting TM2 helices would provide a simple mechanism for triggering conformational changes in HAMP. Despite the broad appeal of this idea (16, 24, 29, 51), there is no experimental evidence for the rotation mechanism in Tar, Tsr, EnvZ, and NarX. Rather, these transducers seem to employ piston-based communication mechanisms (27).

Evidence for the piston mechanism in chemoreceptors has come from comparison of the apo and ligand-bound structures of the Tar periplasmic domain (17), from disulfide formation rates of cysteine reporters in the TM segments of chemoreceptors (28), and from the signaling changes caused by relocating the aromatic and basic anchor residues that secure the position of TM segments in the membrane bilayer (22, 23, 40). Shifts that move TM2 toward the periplasm enhance CW output activity, whereas shifts in the opposite direction enhance CCW signaling. Thus, outward piston movements in chemoreceptors mimic a repellent stimulus, and inward displacements mimic an attractant stimulus. The small vertical displacement is consistent with the free energy change of ligand binding (18, 27).

X-ray structures of nitrate-bound and apo forms of the NarX periplasmic domain revealed an overall structural organization similar to the periplasmic aspartate-binding domain of Tar (18). However, unlike Tar, NarX has only a single binding site at the dimer interface; one bound ligand molecule induces quasi-symmetric conformational changes in both NarX subunits. Nitrate binding causes a small (~1 Å) displacement of both TM2 helices relative to the TM1 helices. However, this piston motion is directed toward the periplasm, in the opposite direction of the aspartate-triggered piston movement in Tar (18). A hybrid transducer (Nart) containing the periplasmic domain of NarX and the kinase control domain of

Tar mediates repellent responses to nitrate and nitrite, consistent with an outward stimulus-induced piston movement (55). A single amino acid change (G51R) in the NarX P box, which contains the ligand-binding determinants (47), changed Nart to an attractant receptor for nitrate (54). These findings suggest that the input control mechanism of HAMP signaling in NarX is similar to that in chemoreceptors.

Output Control Through Phase Clashes

Output control by HAMP domains most likely occurs through their structural connections to adjacent signaling elements. There is no evidence for long-range interactions between HAMP and output regions in other parts of the signaling molecule, a control mechanism suggested by Aravind & Ponting in their defining paper on HAMP (6). Rather, the junctions between AS2 and contiguous output helices provide two important structural clues to a possible general mechanism of HAMP output control (**Figure 4*a***). First, the adjoining output elements are α-helices capable of coiled-coil-like packing interactions. EnvZ and NarX HAMPs connect to helices that interact in a pairwise fashion; the HAMP domains of Tar, Tsr, and Aer, and the HAMP-2 domain of HtrII, connect to helices that form an antiparallel, four-helix bundle (**Figure 4*a***). Second, each of the AS2-output helix junctions in these signaling proteins exhibits a shift of +4 (or −3) residues in heptad repeat register (48, 63), a so-called phase stutter (13, 39) (**Figure 4*a***). Similarly, the linker helix in HtrII comprises an in-phase extension of the AS2–1 helix with a phase stutter at its junction with the AS1–2 helix (not shown). Despite the diversity of output elements in these signaling proteins, the consistent presence of a phase stutter at their junction with AS2 helices makes a strong circumstantial case that HAMP signaling could involve shifts in the packing stability of output helices.

Phase stutter: a +4 (or −3) residue shift in *a-d* packing register of coiled-coils

Phase stutters create an oppositional structural coupling between helical interaction faces. The AS2 helices emerging from a tight HAMP(A) bundle, in either *x-da* or *a-d* configuration, should force adjoining output helices into an unfavorable packing register (**Figure 4*b***). By contrast, loose or altered packing interactions of AS2/AS2′ would allow the output helices to adopt a more stable packing

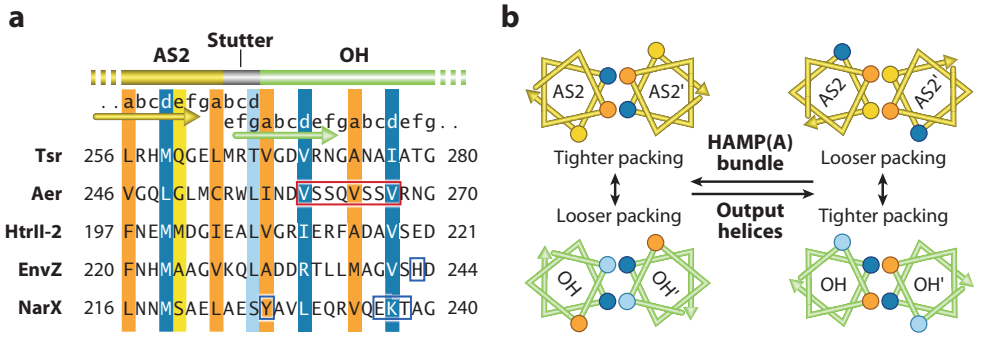

Figure 4

Heptad phase stutters and their structural consequences. (*a*) Junctions of AS2 and output helices (OH); the gray segment is the stutter region. Hydrophobic packing residues in the AS2 and OH segments are labeled in the conventional *a-d* notation for coiled-coils and color coded to the corresponding positions in the helical wheel diagrams in panel *b*. Regions underlined with arrows are shown as helical wheels in panel *b*. Boxed segments identify specific features of output helices discussed in the text. (*b*) Predicted oppositional coupling of AS2/AS2′ and OH1/OH1′ packing interactions. Helical wheels are depicted in the N to C direction and correspond to the segments underlined by arrows in panel *a*. Edge residues that could rotate into the packing interface when the opposing structure is tightly packed are indicated by yellow (AS2) and light blue (OH) symbols and are keyed to their positions in panel *a*.

arrangement (**Figure 4*b***). These structural interactions should operate in both directions. Unstable packing of the output helices would favor a tight HAMP bundle, whereas tight packing of the output helices would favor a loose HAMP bundle. Recent genetic studies, described below, indicate that this mechanistic logic most likely operates in Tsr (63) and in NarX (48).

HAMP SIGNALING IN Tar AND Tsr

Flagellar rotation patterns provide an in vivo readout of receptor signals because the extent of CW rotation is directly related to CheA activity. The flagellar rotation profiles of cell populations having wild-type Tsr as their only chemoreceptor are shown in **Figure 5*a***. In the absence of attractant stimuli, cells without a sensory adaptation system (i.e., lacking the CheR and CheB enzymes) exhibit CW-biased output (**Figure 5*a***). The receptors in CheR$^-$ CheB$^-$ cells have a QEQE modification pattern, in which two of the potential methylation sites are glutamine residues and two are glutamate residues. The glutamine residues mimic the functional properties of glutamyl methyl esters and shift receptors toward a kinase-on state. In adaptation-competent cells, the CheB enzyme converts those glutamines to glutamates in an irreversible deamidation reaction (37, 44). The opposing activities of CheR and CheB then adjust steady-state methylation to a level that offsets ambient attractant concentrations in the environment. In the absence of attractant stimuli, wild-type cells have relatively low MCP methylation levels that produce frequent flagellar reversals, but with an overall CCW-biased signal output (**Figure 5*a***). This output state represents the set point of the adaptation system.

Dynamic Influences on Output Signals

A growing body of evidence links the signaling properties of MCP molecules to their structural stabilities or dynamic motions. Receptor molecules in clustered arrays, for example, seem to freeze or melt in response to stimulus inputs (12), which confers high cooperativity and signal amplification (32). These dynamic effects are best understood for the adaptation region of the MH bundle, where methylation and demethylation changes affect the stability of helix-helix interactions (46, 60). Loosely packed methylation bundles are good substrates for the CheR methyltransferase, which converts target site glutamates to glutamyl methyl esters. Neutralization of the negative charge enhances the packing interactions between methylation helices and serves to stabilize the MH bundle. Conversely, stable MH bundles are good substrates for the CheB methylesterase, which hydrolyzes glutamyl methyl esters to glutamates, creating negative charges along the methylation helices that weaken their interactions.

Stability changes within the MH bundle in turn modulate the packing stability of the receptor's signaling tip (**Figure 1**). Residue changes in the cytoplasmic domain of Tar(St), designed to weaken knob-in-hole helix packing interactions, revealed a yin-yang relationship between helix-packing stability in the adaptation and signaling regions of the Tar molecule (50). Knob truncations at adaptation-region residues often created receptors with locked-off kinase activity, whereas knob truncations at signal-tip residues often created receptors with locked-on kinase activity (50). These findings suggest that the adaptation and signaling regions have structurally opposed stabilities. Enhanced packing of the MH bundle, for example, could weaken helix-packing interactions at the signaling tip. These regions communicate through an intervening flexible bundle and glycine hinge (**Figure 1**), which play an important, but poorly understood, role in receptor signaling (2, 19, 50).

Control Logic of Tsr-HAMP Signaling

Tsr constructs lacking a HAMP domain produce highly CW-biased rotation patterns, whether or not the cells have the CheR and CheB adaptation enzymes (**Figure 5*a***)

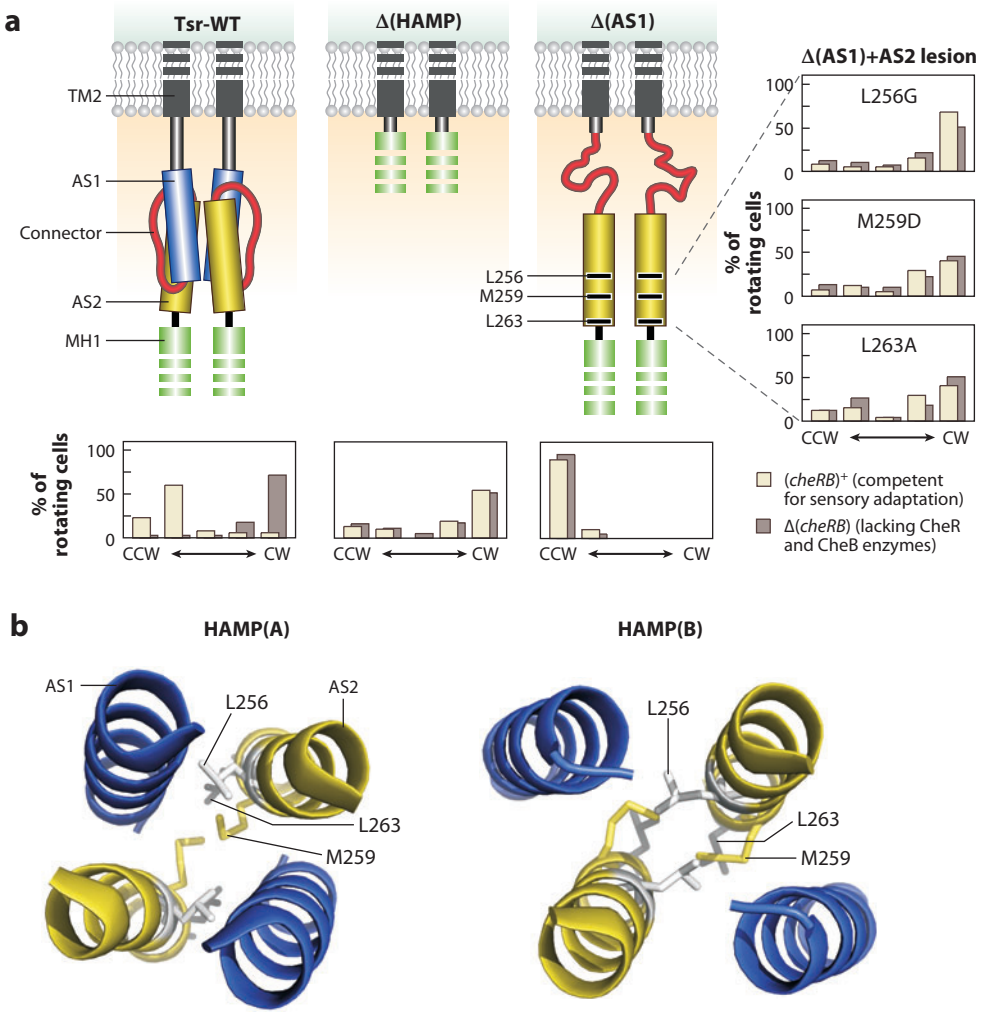

Figure 5

(*a*) Flagellar rotation patterns of wild-type and Tsr HAMP-deletion constructs. Each histogram summarizes the behavior of 100 rotating cells; each cell was observed for 15 s. Each cell was assigned to one of five rotation categories (arranged from left to right): exclusively counterclockwise (CCW); predominantly CCW, but with occasional clockwise (CW) reversals; frequent CW and CCW reversals, with no overall directional bias; predominantly CW, but with occasional CCW reversals; and exclusively CW. Each histogram shows the output behavior of a chemoreceptor in two different genetic backgrounds: one competent for sensory adaptation, $(cheRB)^+$, and one lacking the CheR and CheB enzymes, Δ(*cheRB*). (*b*) Packing alignments of C-terminal AS2 residues in HAMP(A) and HAMP(B) structures. Modeled Tsr-HAMP bundles are viewed in the N to C direction; key hydrophobic side chains are shown as sticks. In HAMP(A) packing, the M259 side chains point toward one another and the center of the bundle. In HAMP(B), the AS2 helices are rotated CCW, allowing the hydrophobic residues to interact in a phase arrangement that would enhance the packing interactions of adjoining output helices.

(P. Ames, Q. Zhou & J.S. Parkinson, unpublished results). The Δ(HAMP) molecules are not substantially modified by either enzyme (P. Ames, Q. Zhou & J.S. Parkinson, unpublished results). Moreover, when their apparent methylation state is mutationally adjusted, for example, to an EEEE or QQQQ pattern, their output remains heavily CW biased (P. Ames, Q. Zhou & J.S. Parkinson, unpublished results). The Δ(HAMP) constructs reveal two important aspects of Tsr-HAMP control. First, the default output state of the Tsr kinase control domain is CW (i.e., kinase-on). The Tsr-HAMP domain is not needed for CheA activation but instead must impose a CCW override that deactivates CheA in response to attractant stimuli. Second, the Tsr-HAMP domain plays an active role in the adaptation process. HAMP-less Tsr molecules are locked in a CW output state, regardless of methylation status, and are poor substrates for CheR and CheB modifications (P. Ames, Q. Zhou & J.S. Parkinson, unpublished results).

Dual CCW Output Signals of Tsr HAMP

A serine stimulus probably elicits a CCW response by enhancing stability of the Tsr-HAMP(A) bundle, which should destabilize the MH bundle (63). CheB-mediated deamidation and demethylation reactions reduce the stability of the MH bundle and should also drive receptors toward the attractant-induced output state, designated CCW(A). However, the flagellar rotation patterns of Tsr-HAMP mutants with structure-destabilizing lesions, for example, polar, charged, or proline replacements at hydrophobic AS1 and AS2 packing residues, reveal another CCW output state, designated CCW(B), which seems to be associated with stable packing of the MH bundle (Q. Zhou, P. Ames & J.S. Parkinson, unpublished results). Two observations indicate that the CCW(B) output effect involves structural interaction of the AS2/AS2′ helices, mediated by their three C-terminal hydrophobic residues. First, amino acid replacements in those AS2 residues cannot produce locked CCW outputs (Q. Zhou, P. Ames & J.S. Parkinson, unpublished results). Second, Δ(AS1) Tsr-HAMP constructs have locked CCW outputs, but amino acid replacements at any of the C-terminal hydrophobic AS2 residues alleviate their CCW behavior (**Figure 5*a***) (P. Ames, Q. Zhou & J.S. Parkinson, unpublished results). HAMP lesions, including Δ(AS1) constructs, that damage the HAMP bundle might allow the AS2 helices to adopt new packing interactions, perhaps similar to those in the HAMP(B) structure (**Figure 3*b***). The C-terminal hydrophobic residues of unconstrained AS2 helices could conceivably contribute to the stability of the MH bundle by adopting the same packing phase (**Figure 5*b***). Such AS2-augmented tight packing of the MH bundle might account for CCW(B) output behavior. The seemingly contradictory conclusion that CCW output occurs at both extremes of the MH bundle stability range argues for a three-state model of Tsr signaling.

A Three-State Model of Tsr Signaling

The dynamic properties of the oppositionally coupled HAMP and MH bundles may control Tsr signal output in a biphasic manner (**Figure 6*a***). When the MH bundle is packed either loose or tight, CheA activity is low and output is CCW. CheA activation (CW output) occurs only in the middle of the MH bundle dynamic range. The adaptation set point of the system lies near the CCW(A) end of the range and defines the midpoint of a physiological operating regime in which the interplay of stimuli and the adaptation system produces a direct relationship between coupled HAMP-MH stability and CheA kinase activity. The signaling behaviors of Tsr-HAMP mutants support this model.

Single amino acid replacements at critical Tsr-HAMP residues cause a variety of mutant output behaviors (Q. Zhou, P. Ames & J.S. Parkinson, unpublished results). The most numerous mutants, including those

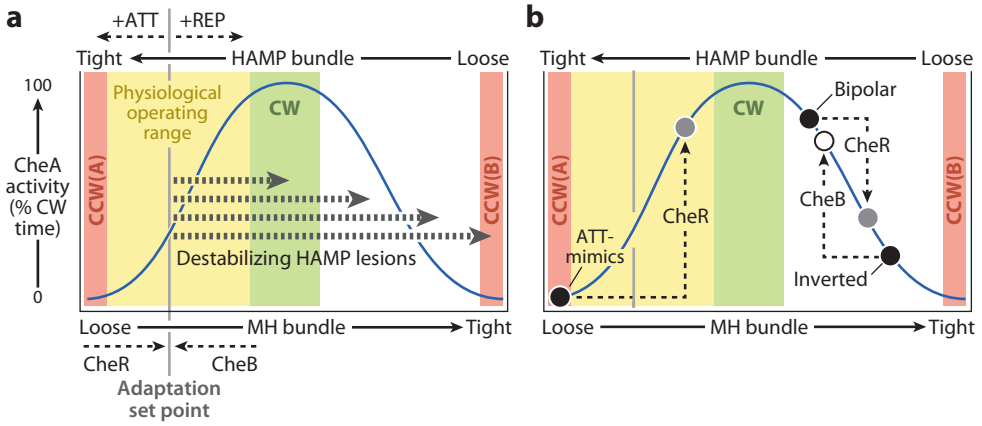

Figure 6

A three-state signaling model for Tsr HAMP. (*a*) Biphasic output diagram of CheA activity versus HAMP and MH bundle packing stability. The system normally operates near the CCW(A) output state, but destabilizing HAMP lesions can drive the system outside this physiological range, leading to aberrant signal outputs, including CW and CCW(B). The precise shape of the blue output curve is not known. (*b*) Biphasic output diagram for three types of Tsr-HAMP mutants: bipolar, inverted, and attractant (ATT)-mimic. Black circles indicate the output activity of the mutant receptors in a *cheR*$^-$ *cheB*$^-$ host lacking both the CheR and CheB adaptation enzymes. Their output signals change in hosts containing one or the other of these enzymes: Gray circles indicate output in a *cheR*$^+$ *cheB*$^-$ host; the white circle indicates output in a *cheR*$^-$ *cheB*$^+$ host. CW, clockwise; CCW, counterclockwise.

with helix-destabilizing proline replacements, exhibit CCW outputs that are refractory to sensory adaptation (Q. Zhou, P. Ames & J.S. Parkinson, unpublished results). The three-state model proposes that these sorts of lesions drive the HAMP bundle to the CCW(B) end of its stability range (see **Figure 6*a***). In contrast, mutants with high CW outputs are much less frequent and seemingly have less structure-perturbing amino acid replacements (e.g., replacement of a critical hydrophobic residue with glycine or with a different hydrophobic amino acid) (Q. Zhou, P. Ames & J.S. Parkinson, unpublished results). The three-state model predicts that CW lesions should cause less drastic HAMP damage, driving bundle stability only slightly outside the physiological range (see **Figure 6*a***).

Other Tsr lesions appear to drive HAMP stability into the region between the CW and CCW(B) regimes and lead to other types of signaling defects, including bipolar and inverted outputs (**Figure 6*b***). Mutant receptors with bipolar outputs produce CW signals in CheR$^-$ CheB$^-$ cells (like the wild type), but CCW outputs in adaptation-competent cells. Mutant receptors with inverted outputs produce CCW signals in CheR$^-$ CheB$^-$ cells, but CW outputs in adaptation-competent cells (3; Q. Zhou, P. Ames & J.S. Parkinson, unpublished results). To determine the individual effects of methylation or deamidation on these unusual signal outputs, mutant receptors were tested in cells having only the CheR or CheB enzyme (Q. Zhou, P. Ames & J.S. Parkinson, unpublished results). Bipolar outputs do not change in CheB$^+$ cells, but become more CCW in CheR$^+$ cells (**Figure 6*b***). Similarly, CheR function does not affect signals from inverted receptors, whereas CheB function shifts them to more CW outputs (**Figure 6*b***). Thus, the output signals of both mutant types respond anomalously to adaptational modification: Methylation drives bipolar receptors to a more CCW output; deamidation drives inverted receptors to a more CW output. These paradoxical

responses are readily explained by a three-state model but are difficult to explain in the context of a two-state signaling model.

Most amino acid replacements at Tsr residues P221 and E248 appear to enhance stability of the HAMP(A) bundle. Lesions at these positions cause CCW-biased outputs in the absence of CheR and CheB, but more wild-type outputs in adaptation-competent hosts (Q. Zhou, P. Ames & J.S. Parkinson, unpublished results). Because CheR alone can drive the mutant receptors to more CW output states, it seems that P221 and E248 lesions mimic the attractant-induced, CCW(A) HAMP signaling state (**Figure 6*b***, ATT-mimics). Lesions at E248 fully abrogate serine-sensing by Tsr, whereas most lesions at P221 only impair Tsr function (63). Cells containing P221 mutant receptors can track serine gradients, although with a reduced detection range, because of the receptors' elevated methylation levels (Q. Zhou, P. Ames & J.S. Parkinson, unpublished results). Conceivably, proline and glutamic acid are conserved at these HAMP positions because they confer an intermediate, rather than maximal, stability to the HAMP(A) bundle. These residues lie close together at the membrane-proximal end of the HAMP(A) bundle and might play a role in initiating HAMP signaling changes in response to stimulus inputs.

Input Control in Tar and Tsr

Tar and Tsr have two symmetric ligand-binding sites at the dimer interface in their periplasmic domains. Binding is negatively cooperative, so receptor dimers usually bind only one ligand molecule, an event that suffices to initiate a signaling response (61). Because ligands can bind in two alternative orientations, stimuli induce an asymmetrical conformation change (61), corresponding to an inward 1–2 Å piston displacement of one TM2 relative to the other (28).

How could a piston motion modulate HAMP signaling activity? In the pushrod-scissors model, a rigid control cable transmits piston displacements to HAMP to cause a scissoring or pivoting motion of the bundle helices (49, 50). In the dynamic bundle model, the control cable exerts tension on the HAMP bundle to modulate its structural stability (63). The pushrod model requires that the control cable be stiff, possibly a stable helix, whereas this is not a requirement of the dynamic bundle model. Although mutational studies in Tsr and Tar have begun to elucidate the nature of the control cable, both models remain in play.

Tsr tolerates insertion or deletion of a single glycine residue in its control cable, but larger insertions and deletions abolish function (P. Ames & J.S. Parkinson, unpublished observations). Deletions enhance CW signal output, evidently mimicking a repellent stimulus; insertions enhance CCW output, mimicking an attractant stimulus. A series of alterations near the start of the AS1 helix in Tar(Ec) have been made to test the importance of helical structure for signal transmission between TM2 and HAMP (M.D. Manson, personal communication). Replacements of four control-cable residues with 1–9 glycines generally mimicked an attractant stimulus, but the three-, four-, and five-glycine replacements retained some signaling ability, suggesting that overall length was a more critical functional factor than specific bundle-packing residues. Similarly, the Tar control cable tolerated deletion of one residue, but not more than one. Additions of glycines or hydrophobic residues near the start of AS1 also impaired function. However, the insertion of four hydrophobic residues allowed the most residual function, hinting that the helical phase of the control cable might also be an important factor in HAMP signaling. These properties of the control cable are compatible with the dynamic bundle model but cannot discount the pushrod-scissors model.

HAMP SIGNALING IN NarX AND EnvZ

Deletions and amino acid replacements in NarX HAMP produce a variety of regulatory

phenotypes that have been monitored through their effects on NarL-dependent induction of a Φ(*narG-lacZ*) reporter (5, 20, 48). Wild-type NarX activates expression about 100-fold upon induction with nitrate or nitrite. Constitutive mutants have high expression levels in the absence of inducer. Elevated basal mutants have high uninduced expression levels but show additional expression increases upon induction. Impaired induction and uninducible mutants have low (i.e., wild-type) basal expression levels but respond incompletely or not at all to inducer. Reversed-response mutants have higher expression levels in the absence than in the presence of inducer.

The Signaling Helix

The NarX HAMP domain controls its kinase and phosphatase output activities through an adjoining S-helix, an ~40-residue motif found in a variety of signaling proteins (4). S-helices contain five heptad repeats that are predicted to form dimeric, parallel coiled-coils. Their defining feature is a central ERT sequence (EKT in NarX), with the basic residue at a *d* heptad position (**Figure 4*a***). The NarX family sensors also have a characteristic tyrosine near the beginning of the S-helix, previously identified as a Y box motif (47). In NarX, there is a phase stutter at the junction of the AS2 and S-helices (**Figure 4*a***) that could produce an oppositional structural coupling of the HAMP and S-helix packing interactions (48).

Stewart & Chen (48) characterized a variety of HAMP and S-helix lesions in NarX that support the idea of phase-clash control. Several seven-residue deletions in the stutter region, which would not alter the AS2/S-helix phase relationship, produced a constitutive phenotype. In contrast, two four-residue deletions, which precisely ablate the stutter, caused an uninducible phenotype, as did two seven-residue deletions spanning the S-helix EKT motif. These control defects could reflect changes in the structural interplay between HAMP and S-helix packing stabilities. Removal of the phase stutter could conceivably enhance the packing stability of the S-helix, perhaps driving the overall dynamic behavior of the coupled system outside the stimulus-responsive range. Although the structural role of the EKT motif is less clear, it could conceivably serve to weaken the S-helix packing interactions, thereby rendering them sensitive to HAMP manipulation. Thus, removal of the EKT residues might tighten S-helix packing, perhaps with a concomitant loosening of the HAMP bundle. These behaviors are reminiscent of the CCW(B) output state in Tsr.

Heptad-length deletions in the AS1 and connector elements of NarX HAMP cause constitutive phenotypes, but often with some residual responsiveness to nitrate stimuli (5, 48). Deletions and amino acid replacements in AS2 produced both constitutive and reversed-response behaviors. Thus, the NarX AS2 helices seem to play important roles in controlling both basal and stimulus-induced output signals. Perhaps, like their counterparts in Tsr, the C-terminal hydrophobic AS2 residues in NarX HAMP contribute to two kinase-off signaling states.

A Working Model for NarX Signaling

NarX HAMP mutants with reversed responses to ligands, which behave much like the inverted mutants of Tsr HAMP, imply a biphasic relationship between kinase activity and the dynamic behavior of the HAMP/S-helix duo. Conceivably, NarX has kinase-off states at each end of its stability spectrum, analogous to the CCW(A) and CCW(B) states of Tsr. The NarX set point might be close to the kinase-off state predicted for a tight HAMP(A) bundle. Stimuli could destabilize HAMP(A), driving it into a more dynamic range with high kinase activity. Evidently, many destabilizing lesions in NarX HAMP also drive the system into the high kinase range. Perhaps the intrinsic instability of the S-helix prevents such lesions from driving the system past the high kinase range. However, removal of the phase stutter or the EKT

Phase clash: incompatible packing arrangements of coiled-coil segments on either side of a phase stutter; causes an oppositional coupling of structural stabilities

motif might enhance S-helix stability enough to drive the system into a second kinase-off state, yielding an uninducible signaling phenotype.

HAMP Signaling in EnvZ

EnvZ HAMP is best understood at the input control step, mainly based on studies of chimeric transducers, which first demonstrated that HAMP converts asymmetric conformational inputs to symmetric signal outputs (61, 65). Taz1 and Tez1 contain the output domain of EnvZ fused to the aspartate-binding domain of Tar (53, 64). Taz1 is spliced near the C terminus of HAMP; Tez1 is spliced in the control cable. In both transducers, an aspartate stimulus enhances EnvZ kinase activity, suggesting that, like Tar, the EnvZ-sensing domain might transmit stimulus information through inward TM piston motions. The Tez1 chimera has an uninducible phenotype, presumably owing to the different lengths of the Tar and EnvZ control cables. However, addition of an alanine residue to the Tez1 control cable provided regulated control, and addition of a second alanine produced a constitutive phenotype (64). These findings confirm that piston motions can modulate EnvZ-HAMP signaling. Like NarX, most EnvZ HAMP lesions produce constitutive kinase activity, implying a similar signaling logic (36, 41, 64). However, unlike NarX, inward piston motions seem to induce EnvZ kinase activity, suggesting that EnvZ-HAMP may operate near the loose-packing end of the HAMP stability range in a three-state signaling scheme.

HAMP SIGNALING IN Aer AND HtrII

Output Control in Aer

Aer contains a phase stutter at the C terminus of AS2 (**Figure 4*a***), but unlike in Tar and Tsr, this transition zone is not the epicenter of destabilizing phase clashes between the HAMP and methylation helices. Rather, disulfide cross-linking studies indicate that the AS2 phase arrangement continues through the stutter and the first three residues of MH1 (56). Moreover, cysteine replacements at two stutter residues abrogated Aer function: W255C caused a CW output bias; L256C caused a null (CCW) phenotype (56). These defects suggest that the AS2 packing phase is important for Aer signaling and that the stutter residues contribute to its stability.

Disulfide cross-linking studies also revealed a loop in the Aer MH bundle from V260-V267 (**Figure 4*a***), followed by a continuation of the *a-d* heptad phase of AS2, with numerous polar residues at the MH packing positions (56). These patterns suggest that in Aer the HAMP(A) bundle is relatively more stable than the MH bundle and dominates the packing phase over an extended transition zone. The loop might represent a region with low helix-forming potential, perhaps comparable to a proteolytically sensitive region at the AS2-MH1 junction in Tar(St) (49). The signaling properties of Aer-Tar hybrids indicate that the loop residues of Aer influence MH bundle stability differently than their counterparts in Tar or Tsr. Some chimeric transducers with the PAS-HAMP portion of Aer and the kinase control domain of Tar exhibit methylation-mediated sensory adaptation to aerotactic stimuli, whereas others do not (9).

CW-biased lesions in the Aer PAS domain altered cross-linking behavior in several ways, presumably reflecting structural changes in the HAMP domain upon CW signaling (K. Watts, personal communication). Some cross-links at the top of the bundle formed less readily, whereas some at the bottom of the bundle formed more readily. The CW signaling state also showed increased vertical movements of the AS1 and AS2 helices (K. Watts, personal communication). These changes are at least consistent with a transition to a looser HAMP bundle upon CW signaling.

Input Control in Aer

The PAS domain of Aer is essential for CW output, even in chimeric transducers that have Tar

or Tsr kinase control domains (K. Gosink & J.S. Parkinson, unpublished observations). Aer molecules lacking a PAS domain also cannot acquire CheA-activating ability through single mutational alterations of the kinase control domain (K. Gosink & J.S. Parkinson, unpublished observations). These findings suggest that a PAS domain with its FAD cofactor in a reduced state activates CW output through interaction with the Aer HAMP domain. Oxidation of the FAD cofactor triggers a conformational change in PAS that stops the CW signal, initiating an aerotactic response. Two lines of evidence suggest that the Aer PAS domain may interact with the output end of the HAMP bundle and the proximal MH segments: (*a*) An amino acid replacement at the C terminus of AS2 (C253R) is phenotypically suppressed by a specific PAS alteration (N34D) (57); and (*b*) many CW-biased Aer-HAMP lesions cluster at the output end of the HAMP bundle (56).

Lesions that enhance the CW output of Aer still require the PAS domain for CW output (K. Gosink & J.S. Parkinson, unpublished observations), suggesting that they act by promoting the CW-generating PAS-HAMP interaction. CW-biased Aer HAMP lesions (14, 56, 57) have counterparts in Tsr-HAMP (3; Q. Zhou, P. Ames & J.S. Parkinson, unpublished results) and most likely reduce the stability of the HAMP(A) bundle (3, 63). These CW HAMP lesions may enhance formation of an alternative HAMP conformation that has high affinity for the PAS domain. Upon PAS/FAD binding, that HAMP structure presumably undergoes additional changes that modulate the stability of the Aer MH bundle and kinase control domain to activate the CheA kinase.

Aer is the best-studied example of a transducer that triggers stimulus responses through direct cytoplasmic sensory input to the HAMP domain. A recently described family of bipartite energy taxis receptors also employs this signaling route, but with two separate proteins: a PAS-containing sensor and a HAMP-containing signaler (25, 26). Evidently, a covalent connection between PAS and HAMP is not a critical feature of this input mode.

HAMP Signaling in HtrII

Sensory rhodopsin II forms a stable membrane complex with HtrII through structural interactions of their transmembrane helices (30, 62). Light triggers conformational changes in SRII that induce a 15° CCW rotation of HtrII-TM2 (viewed from the periplasm toward the cytoplasm) (58). Assuming that the connection between TM2 and the first HtrII HAMP domain is sufficiently rigid, CCW rotation of the AS1 helices would reduce the stability of a HAMP(A) bundle by shifting critical hydrophobic residues away from the packing interface (**Figure 2*b***). In fact, blue light stimuli trigger a conformational change in the first HAMP domain of HtrII that is consistent with increased solvent exposure of the AS1 helices (35).

The signaling role of the second HAMP domain in HtrII is unclear. Moderate destabilization of a single HAMP(A) bundle would be expected to shift the receptor to kinase-activating output (63; Q. Zhou, P. Ames & J.S. Parkinson, unpublished results), which should suffice for a photophobic behavioral response. However, if the second HtrII HAMP domain operated mainly as a HAMP(B) bundle, its structural stability would be reinforced by a phase-stutter connection to a stable N-terminal HAMP(A) domain. Conversely, destabilization of the HAMP(A) domain should reduce stability of the stutter-coupled HAMP(B) domain. Perhaps tandem HAMP domains in opposing structural states comprise bistable switching units that exhibit more all-or-none response behavior than single HAMP domains do.

The HtrII(Np) transducer appears to employ the crankshaft mechanism for HAMP input control, although there may also be a piston component to the light-induced TM2 motion. HtrII(Hs) has a periplasmic domain that senses serine as a chemoattractant (33). It may be that both rotational and piston motions can

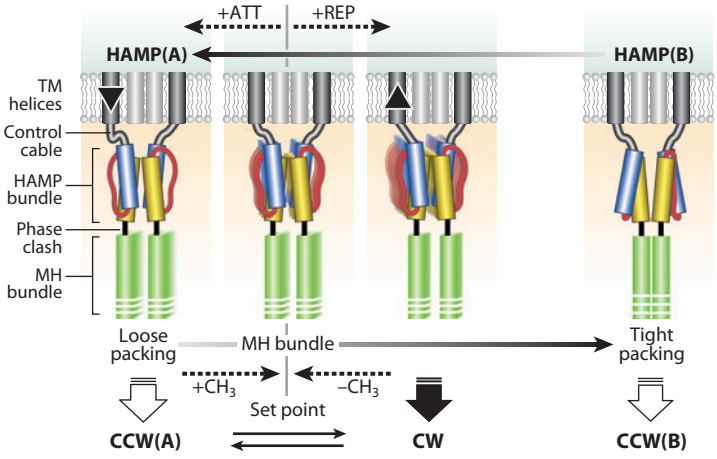

Figure 7

Dynamic bundle model of HAMP signaling in Tsr. The greater the number of shadow images for a particular structural element, the looser its packing. HAMP domains may adopt two alternative conformations, HAMP(A) and HAMP(B), both of which cause CCW output in Tsr. When the two HAMP structures rapidly interconvert, or when neither is stable, output is CW. The HAMP(A) conformation seems to predominate in Tsr. In Tsr, attractant stimuli cause a small inward displacement of one TM2 segment (*downward-pointing triangle*); repellent stimuli cause outward displacement of one TM2 segment (*upward-pointing triangle*). Stimuli and methylation state probably shift signal output by influencing the stability of the HAMP(A) structure. Similar mechanisms may operate in other chemoreceptors and in sensor kinases, using any portion of the overall HAMP(A)-HAMP(B) dynamic range. Abbreviations: CW, clockwise; CCW, counterclockwise; MH, methylation helices; TM, transmembrane helix.

modulate HAMP signal output in the same transducer. Comparison of light- and serine-induced conformational changes in HtrII(Hs) could elucidate this important mechanistic issue.

A DYNAMIC BUNDLE VIEW OF HAMP SIGNALING

In the three-state Tsr signaling model the CW (kinase-on) output state corresponds to multiple conformations in the middle of the HAMP bundle dynamic range (63). One way the system could work is through oscillation of the HAMP bundle between the HAMP(A) and HAMP(B) conformational states (**Figure 7**). Stimuli could elicit signaling changes by shifting the relative stabilities of those two HAMP structures. Although the dynamic operating ranges of Tsr and NarX seem to be dominated by the HAMP(A) structure, lesions that reduce HAMP(A) stability reveal the underlying contribution of a HAMP(B)-like structure to their signaling behavior. Other HAMP-containing transducers might use a similar three-state signaling mechanism, which in principle could operate over any portion of the HAMP dynamic range.

SUMMARY POINTS

1. Stimulus-induced conformational changes can be conveyed to HAMP domains through piston (Tar, Tsr, NarX, EnvZ) or rotary (HtrII) motions of adjoining transmembrane helices or through direct interaction with a cytoplasmic sensing domain (Aer).
2. Input stimuli probably modulate HAMP signaling by shifting the relative stabilities of alternative HAMP structural states, designated HAMP(A) and HAMP(B), both of which may generate kinase-off output states. Thus, control of output kinase activity could involve changes in the dynamic behavior of one or both HAMP conformations.
3. HAMP domains probably control the output activities of signaling proteins by modulating the packing stabilities of the output helices through oppositional structural coupling.
4. Output control may involve helical phase clashes caused by a stutter arrangement of hydrophobic packing residues at the junction between output helices and the AS2/AS2′ helices of HAMP.

5. The kinase-on states of chemoreceptors and sensor kinases probably occur over an intermediate range of HAMP stabilities and dynamic behaviors. Output helices that are too tightly or too loosely packed most likely produce kinase-off output states.
6. A three-state, dynamic bundle signaling model best accounts for the signaling properties of Tsr and NarX HAMP mutants and may apply to other transducers as well.

DISCLOSURE STATEMENT

The author is not aware of any affiliations, memberships, funding, or financial holdings that might be perceived as affecting the objectivity of this review.

ACKNOWLEDGMENTS

Many thanks to the following colleagues for providing ideas, preprints, and/or comments on drafts of this article: Michael Airola and Brian Crane, Joe Falke, Andrei Lupas, Mike Manson, Joachim Schultz, John Spudich, Valley Stewart, Claudia Studdert, and Kylie Watts. Michael Airola and Brian Crane also provided atomic coordinates for Aer2 HAMP structures and a threaded Tsr structure. Research in my lab is funded by grant GM19559 from the National Institute of General Medical Sciences.

LITERATURE CITED

1. **Airola M, Watts KJ, Crane BR. 2010. Structure of concatenated HAMP domains provides a mechanism for signal transduction. *Structure* 18:436–48**
2. Alexander RP, Zhulin IB. 2007. Evolutionary genomics reveals conserved structural determinants of signaling and adaptation in microbial chemoreceptors. *Proc. Natl. Acad. Sci. USA* 104:2885–90
3. Ames P, Zhou Q, Parkinson JS. 2008. Mutational analysis of the connector segment in the HAMP domain of Tsr, the *Escherichia coli* serine chemoreceptor. *J. Bacteriol.* 190:6676–85
4. Anantharaman V, Balaji S, Aravind L. 2006. The signaling helix: a common functional theme in diverse signaling proteins. *Biol. Direct.* 1:25. doi: 10.1186/1745-6150-1-25
5. Appleman JA, Stewart V. 2003. Mutational analysis of a conserved signal-transducing element: the HAMP linker of the *Escherichia coli* nitrate sensor NarX. *J. Bacteriol.* 185:89–97
6. **Aravind L, Ponting CP. 1999. The cytoplasmic helical linker domain of receptor histidine kinase and methyl-accepting proteins is common to many prokaryotic signaling proteins. *FEMS Microbiol. Lett.* 176:111–16**
7. Bibikov SI, Barnes LA, Gitin Y, Parkinson JS. 2000. Domain organization and flavin adenine dinucleotide-binding determinants in the aerotaxis signal transducer Aer of *Escherichia coli*. *Proc. Natl. Acad. Sci. USA* 97:5830–35
8. Bibikov SI, Biran R, Rudd KE, Parkinson JS. 1997. A signal transducer for aerotaxis in *Escherichia coli*. *J. Bacteriol.* 179:4075–79
9. Bibikov SI, Miller AC, Gosink KK, Parkinson JS. 2004. Methylation-independent aerotaxis mediated by the *Escherichia coli* Aer protein. *J. Bacteriol.* 186:3730–37
10. Boldog T, Hazelbauer GL. 2004. Accessibility of introduced cysteines in chemoreceptor transmembrane helices reveals boundaries interior to bracketing charged residues. *Protein Sci.* 13:1466–75
11. Bordignon E, Klare JP, Doebber M, Wegener AA, Martell S, et al. 2005. Structural analysis of a HAMP domain: the linker region of the phototransducer in complex with sensory rhodopsin II. *J. Biol. Chem.* 280:38767–75

1. Presents the structures of three concatenated HAMP domains, including the first description of the HAMP(B) conformational state.

6. One of two papers that explicitly defined the HAMP domain (see also Reference 59).

12. Bray D, Williams D. 2008. How the "melting" and "freezing" of protein molecules may be used in cell signaling. *ACS Chem. Biol.* 3:89–91
13. Brown JH, Cohen C, Parry DA. 1996. Heptad breaks in alpha-helical coiled coils: stutters and stammers. *Proteins* 26:134–45
14. Buron-Barral MC, Gosink KK, Parkinson JS. 2006. Loss- and gain-of-function mutations in the F1-HAMP region of the *Escherichia coli* aerotaxis transducer Aer. *J. Bacteriol.* 188:3477–86
15. Butler SL, Falke JJ. 1998. Cysteine and disulfide scanning reveals two amphiphilic helices in the linker region of the aspartate chemoreceptor. *Biochemistry* 37:10746–56
16. Casino P, Rubio V, Marina A. 2009. Structural insight into partner specificity and phosphoryl transfer in two-component signal transduction. *Cell* 139:325–36
17. Chervitz SA, Falke JJ. 1996. Molecular mechanism of transmembrane signaling by the aspartate receptor: a model. *Proc. Natl. Acad. Sci. USA* 93:2545–50
18. Cheung J, Hendrickson WA. 2009. Structural analysis of ligand stimulation of the histidine kinase NarX. *Structure* 17:190–201
19. Coleman MD, Bass RB, Mehan RS, Falke JJ. 2005. Conserved glycine residues in the cytoplasmic domain of the aspartate receptor play essential roles in kinase coupling and on-off switching. *Biochemistry* 44:7687–95
20. Collins LA, Egan SM, Stewart V. 1992. Mutational analysis reveals functional similarity between NarX, a nitrate sensor in *Escherichia coli* K-12, and the methyl-accepting chemotaxis proteins. *J. Bacteriol.* 174:3667–75
21. Doebber M, Bordignon E, Klare JP, Holterhues J, Martell S, et al. 2008. Salt-driven equilibrium between two conformations in the HAMP domain from *Natronomonas pharaonis*: the language of signal transfer? *J. Biol. Chem.* 283:28691–701
22. Draheim RR, Bormans AF, Lai RZ, Manson MD. 2005. Tryptophan residues flanking the second transmembrane helix (TM2) set the signaling state of the Tar chemoreceptor. *Biochemistry* 44:1268–77
23. Draheim RR, Bormans AF, Lai RZ, Manson MD. 2006. Tuning a bacterial chemoreceptor with protein-membrane interactions. *Biochemistry* 45:14655–64
24. Dunin-Horkawicz S, Lupas AN. 2010. Comprehensive analysis of HAMP domains: implications for transmembrane signal transduction. *J. Mol. Biol.* 397:1156–74
25. Elliott KT, Dirita VJ. 2008. Characterization of CetA and CetB, a bipartite energy taxis system in *Campylobacter jejuni*. *Mol. Microbiol.* 69:1091–103
26. Elliott KT, Zhulin IB, Stuckey JA, DiRita VJ. 2009. Conserved residues in the HAMP domain define a new family of proposed bipartite energy taxis receptors. *J. Bacteriol.* 191:375–87
27. Falke JJ, Erbse AH. 2009. The piston rises again. *Structure* 17:1149–51
28. Falke JJ, Hazelbauer GL. 2001. Transmembrane signaling in bacterial chemoreceptors. *Trends. Biochem. Sci.* 26:257–65
29. Gao R, Stock AM. 2009. Biological insights from structures of two-component proteins. *Annu. Rev. Microbiol.* 63:133–54
30. Gordeliy VI, Labahn J, Moukhametzianov R, Efremov R, Granzin J, et al. 2002. Molecular basis of transmembrane signaling by sensory rhodopsin II-transducer complex. *Nature* 419:484–87
31. Hayashi K, Sudo Y, Jee J, Mishima M, Hara H, et al. 2007. Structural analysis of the phototactic transducer protein HtrII linker region from *Natronomonas pharaonis*. *Biochemistry* 46:14380–90
32. Hazelbauer GL, Falke JJ, Parkinson JS. 2008. Bacterial chemoreceptors: high-performance signaling in networked arrays. *Trends. Biochem. Sci.* 33:9–19
33. Hou S, Brooun A, Yu HS, Freitas T, Alam M. 1998. Sensory rhodopsin II transducer HtrII is also responsible for serine chemotaxis in the archaeon *Halobacterium salinarum*. *J. Bacteriol.* 180:1600–2
34. Hulko M, Berndt F, Gruber M, Linder JU, Truffault V, et al. 2006. The HAMP domain structure implies helix rotation in transmembrane signaling. *Cell* 126:929–40
35. Inoue K, Sasaki J, Spudich JL, Terazima M. 2008. Signal transmission through the HtrII transducer alters the interaction of two alpha-helices in the HAMP domain. *J. Mol. Biol.* 376:963–70
36. Jin T, Inouye M. 1994. Transmembrane signaling. Mutational analysis of the cytoplasmic linker region of Taz1-1, a Tar-EnvZ chimeric receptor in *Escherichia coli*. *J. Mol. Biol.* 244:477–81

28. Summarizes the experimental evidence in support of the piston model of transmembrane signaling in chemoreceptors.

32. Provides an up-to-date summary of chemoreceptor structure and function.

34. Reports the first HAMP structure to be determined and proposes the crankshaft and gearbox model of transmembrane signaling.

37. Kehry MR, Bond MW, Hunkapiller MW, Dahlquist FW. 1983. Enzymatic deamidation of methyl-accepting chemotaxis proteins in *Escherichia coli* catalyzed by the *cheB* gene product. *Proc. Natl. Acad. Sci. USA* 80:3599–603
38. Kishii R, Falzon L, Yoshida T, Kobayashi H, Inouye M. 2007. Structural and functional studies of the HAMP domain of EnvZ, an osmosensing transmembrane histidine kinase in *Escherichia coli*. *J. Biol. Chem.* 282:26401–8
39. Lupas A. 1996. Coiled coils: new structures and new functions. *Trends Biochem. Sci.* 21:375–82
40. Miller AS, Falke JJ. 2004. Side chains at the membrane-water interface modulate the signaling state of a transmembrane receptor. *Biochemistry* 43:1763–70
41. Park H, Inouye M. 1997. Mutational analysis of the linker region of EnvZ, an osmosensor in *Escherichia coli*. *J. Bacteriol.* 179:4382–90
42. Rebbapragada A, Johnson MS, Harding GP, Zuccarelli AJ, Fletcher HM, et al. 1997. The Aer protein and the serine chemoreceptor Tsr independently sense intracellular energy levels and transduce oxygen, redox, and energy signals for *Escherichia coli* behavior. *Proc. Natl. Acad. Sci. USA* 94:10541–46
43. Repik A, Rebbapragada A, Johnson MS, Haznedar JO, Zhulin IB, Taylor BL. 2000. PAS domain residues involved in signal transduction by the Aer redox sensor of *Escherichia coli*. *Mol. Microbiol.* 36:806–16
44. Rice MS, Dahlquist FW. 1991. Sites of deamidation and methylation in Tsr, a bacterial chemotaxis sensory transducer. *J. Biol. Chem.* 266:9746–53
45. Sasaki J, Spudich JL. 2008. Signal transfer in haloarchaeal sensory rhodopsin-transducer complexes. *Photochem. Photobiol.* 84:863–68
46. Starrett DJ, Falke JJ. 2005. Adaptation mechanism of the aspartate receptor: electrostatics of the adaptation subdomain play a key role in modulating kinase activity. *Biochemistry* 44:1550–60
47. Stewart V. 2003. Biochemical Society Special Lecture. Nitrate- and nitrite-responsive sensors NarX and NarQ of proteobacteria. *Biochem. Soc. Trans.* 31:1–10
48. Stewart V, Chen LL. 2010. The S-helix mediates signal transmission as a HAMP domain coiled-coil extension in the NarX nitrate sensor from *Escherichia coli* K-12. *J. Bacteriol.* 192:734–45
49. Swain KE, Falke JJ. 2007. Structure of the conserved HAMP domain in an intact, membrane-bound chemoreceptor: a disulfide mapping study. *Biochemistry* 46:13684–95
50. Swain KE, Gonzalez MA, Falke JJ. 2009. Engineered socket study of signaling through a four-helix bundle: evidence for a yin-yang mechanism in the kinase control module of the aspartate receptor. *Biochemistry* 48:9266–77
51. Szurmant H, White RA, Hoch JA. 2007. Sensor complexes regulating two-component signal transduction. *Curr. Opin. Struct. Biol.* 17:706–15
52. Taylor BL. 2007. Aer on the inside looking out: paradigm for a PAS-HAMP role in sensing oxygen, redox and energy. *Mol. Microbiol.* 65:1415–24
53. Utsumi R, Brissette RE, Rampersaud A, Forst SA, Oosawa K, Inouye M. 1989. Activation of bacterial porin gene expression by a chimeric signal transducer in response to aspartate. *Science* 245:1246–49
54. Ward SM, Bormans AF, Manson MD. 2006. Mutationally altered signal output in the Nart (NarX-Tar) hybrid chemoreceptor. *J. Bacteriol.* 188:3944–51
55. Ward SM, Delgado A, Gunsalus RP, Manson MD. 2002. A NarX-Tar chimera mediates repellent chemotaxis to nitrate and nitrite. *Mol. Microbiol.* 44:709–19
56. Watts KJ, Johnson MS, Taylor BL. 2008. Structure-function relationships in the HAMP and proximal signaling domains of the aerotaxis receptor Aer. *J. Bacteriol.* 190:2118–27
57. Watts KJ, Ma Q, Johnson MS, Taylor BL. 2004. Interactions between the PAS and HAMP domains of the *Escherichia coli* aerotaxis receptor Aer. *J. Bacteriol.* 186:7440–49
58. Wegener AA, Klare JP, Engelhard M, Steinhoff HJ. 2001. Structural insights into the early steps of receptor-transducer signal transfer in archaeal phototaxis. *EMBO J.* 20:5312–19
59. Williams SB, Stewart V. 1999. Functional similarities among two-component sensors and methyl-accepting chemotaxis proteins suggest a role for linker region amphipathic helices in transmembrane signal transduction. *Mol. Microbiol.* 33:1093–102
60. Winston SE, Mehan R, Falke JJ. 2005. Evidence that the adaptation region of the aspartate receptor is a dynamic four-helix bundle: cysteine and disulfide scanning studies. *Biochemistry* 44:12655–66

48. Presents evidence for a phase stutter and dynamic bundle control of signal output in NarX.

59. Explicitly defines the HAMP domain (see also Reference 6).

61. Yang Y, Park H, Inouye M. 1993. Ligand binding induces an asymmetrical transmembrane signal through a receptor dimer. *J. Mol. Biol.* 232:493–98
62. Zhang XN, Zhu J, Spudich JL. 1999. The specificity of interaction of archaeal transducers with their cognate sensory rhodopsins is determined by their transmembrane helices. *Proc. Natl. Acad. Sci. USA* 96:857–62
63. Zhou Q, Ames P, Parkinson JS. 2009. Mutational analyses of HAMP helices suggest a dynamic bundle model of input-output signaling in chemoreceptors. *Mol. Microbiol.* 73:801–14
64. Zhu Y, Inouye M. 2003. Analysis of the role of the EnvZ linker region in signal transduction using a chimeric Tar/EnvZ receptor protein, Tez1. *J. Biol. Chem.* 278:22812–19
65. Zhu Y, Inouye M. 2004. The HAMP linker in histidine kinase dimeric receptors is critical for symmetric transmembrane signal transduction. *J. Biol. Chem.* 279:48152–58

63. Describes an extensive mutational analysis of the Tsr HAMP domain, develops the concept of oppositional structural coupling via phase stutters, and presents evidence and arguments for a dynamic bundle model of HAMP signaling.

Annual Review of Microbiology
Volume 64, 2010

Contents